

Competition between polaron pair formation and singlet fission observed in amorphous rubrene films

Vygintas Jankus,^{1,*} Edward W. Snedden,¹ Daniel W. Bright,¹ Erhan Arac,² DeChang Dai,¹ and Andrew P. Monkman¹

¹*Physics Department, Durham University, South Road, Durham, DH1 3LE, United Kingdom*

²*School of Electrical and Electronic Engineering, Newcastle upon Tyne, NE1 7RU, United Kingdom*

(Received 9 October 2012; revised manuscript received 5 April 2013; published 4 June 2013)

In this paper, we investigate excited state dynamics in amorphous rubrene vacuum sublimed films. We report the direct observation of singlet fission in amorphous rubrene films. We have determined the fission rate to be $>2.5 \times 10^{12} \text{ s}^{-1}$. Simultaneously, we observe strong polaron pair absorption and propose that polaron pair formation could be competing with singlet fission. Another possible conclusion from our experiments could be that two triplets from singlet fission might arise via polaron pairs. In either case, polaron pairs play an important role in singlet fission in an amorphous rubrene film. We also observe that triplets created by singlet fission fuse to regenerate a singlet, giving delayed fluorescence (DF) scaling linearly with initial laser energy (i.e., one singlet gives two triplets and two triplets give back one singlet). This is a strong evidence of $S_1^n \rightarrow 2T_1$. We did not observe substantial temperature dependence of DF decay curve shape, indicating that triplet migration in amorphous rubrene films is not hopping limited and that triplets undergo fusion before their migration.

DOI: [10.1103/PhysRevB.87.224202](https://doi.org/10.1103/PhysRevB.87.224202)

PACS number(s): 78.47.da, 78.47.jb, 78.47.jd, 78.55.Kz

I. INTRODUCTION

It has been suggested that triplet excitons could be harvested to give charges in bulk heterojunction or even bilayer organic solar cells.¹ For this, large triplet diffusion lengths are highly beneficial. Rubrene could be an excellent candidate, because it has been shown that triplets can diffuse in the range of micrometers in single rubrene crystals.^{2,3} Long diffusion length triplet excitons would allow them to reach far interfaces so that more efficient charge separation could take place. Furthermore, if triplets could be created via singlet fission, the number of excitons created per photon, and potentially the efficiency of organic solar cells, could be doubled. As in tetracene,^{4,5} it has been suggested that singlets in rubrene undergo fission into two triplets.^{2,6,7} The lowest energy rubrene triplet level has been reported to be between 1.14–1.15 and 1.04–1.05 eV (in solution). Triplet energy level value has not been measured in film or crystal. The singlet is between 2.21 and 2.29 eV (in solution), so singlet fission should be isoenergetic or slightly endothermic.^{8–10} Most of the previous investigations have been made on crystalline rubrene, which is difficult to deposit and use in practical applications.^{6,7} In this paper, we report the direct observation of singlet fission in rubrene amorphous thin films (40–120 nm) grown via a simple vacuum sublimation technique, and we have used femtosecond and nanosecond spectroscopy to explore the photophysical properties of excited state dynamics in these films. We also investigate triplet-triplet annihilation in these films.

II. EXPERIMENTAL DETAILS

Rubrene was thermally evaporated using a commercial Kurt Lesker Spectros II deposition system consisting of a vacuum (down to 10^{-7} mbar) chamber, six low-temperature organic evaporation sources, three metal evaporation sources, quartz sensors to measure the deposition rate and thickness of evaporation, and a substrate holder, which is normally rotated during the evaporation. Sublimed grade rubrene (99.99%) was

purchased from Aldrich and used without further purification. Thin films were evaporated at 0.3 Å/s onto sapphire substrates 12 mm in diameter. Sample thickness (40–120 nm) was measured using a J. A. Woollam ellipsometer (Cauchy fitting). The surface morphology and crystal structure of our films were investigated using atomic force microscopy (AFM) and x-ray diffraction (XRD), respectively. AFM measurements were performed in noncontact mode with the scan rate of 0.5 Hz. The XRD measurements were performed using a Bede D1 diffractometer. All samples were measured just after evaporation in a vacuum below 10^{-4} mbar.

For ultrafast transient absorption spectroscopy, a conventional noncollinear pump-probe setup was employed. The output of a Ti:sapphire femtosecond oscillator (Coherent Mira900-f, 1.6 eV, 180 fs, 6 nJ, 76 MHz), used in conjunction with a Ti:sapphire femtosecond amplifier (Coherent RegA 9000, 180 fs, 5 μ J, 100 kHz) was used to drive a opto-parametric amplifier (Coherent 9400-OPA) and create both excitation (3.2 eV) and probe (white-light supercontinuum, 1.24–2.64 eV) sources. The variable delay between pump and probe pulses was controlled by means of a motorized linear translation stage (Newport, 600 mm). A variable $\lambda/4$ waveplate was used to orient excitation and probe pulses under magic angle (54.7°) conditions to remove polarization artifacts. Spectral components in the white-light probe were resolved using a monochromator (Bentham M300) prior to detection, with the relative transmission change $\Delta T/T$ of the probe measured using an amplified silicon photodiode in conjunction with a phase-sensitive lock-in technique.

Gated luminescence and lifetime measurements were made using a system consisting of excitation source, pulsed (150-ps width) yttrium aluminum garnet laser emitting at 355 or 532 nm (Ekspla). Samples were excited at a 45° angle to the substrate plane, and the energy of each pulse could be tuned from microjoules up to millijoules. Emission was focused onto a spectrograph and detected on a sensitive gated intensified charge-coupled device camera (Stanford Computer Optics)

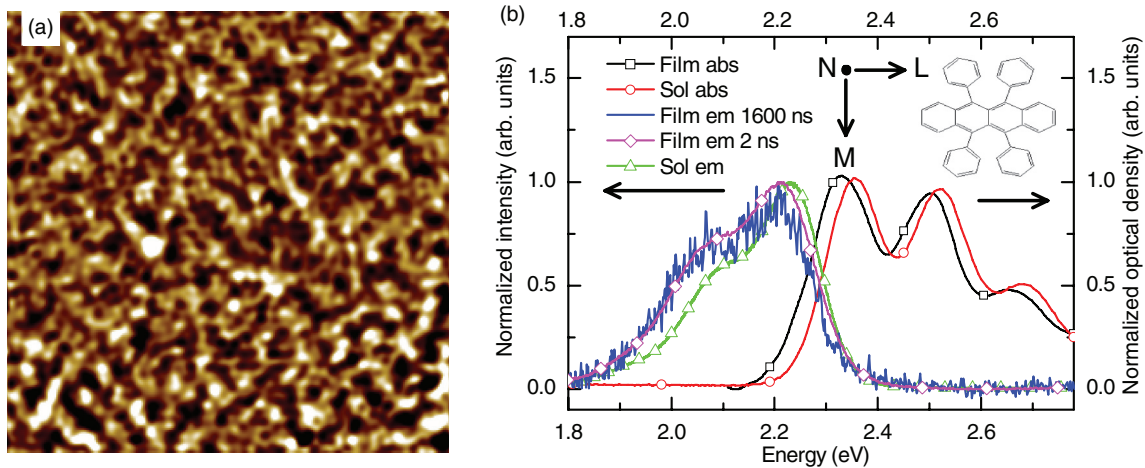


FIG. 1. (Color online) (a) $5 \times 5 \mu\text{m}^2$ AFM image of evaporated rubrene film on sapphire. (b) Normalized absorption and emission of sublimed rubrene film and rubrene in toluene solution (4×10^{-5} M) at room temperature. Rubrene film emission curves were recorded 2 ns after excitation (PF) and 1600 ns after excitation (DF). Inset: rubrene molecular structure and orientations N , M , and L .

with subnanosecond resolution. Decay measurements were performed by logarithmically increasing gate and delay times; more details can be found elsewhere.¹¹ For low-temperature measurements (down to 12 K), samples were placed in a cryostat. Steady state absorption of films was recorded using a ultraviolet-visible spectrophotometer (UV-VIS 3600 from Shimadzu).

III. RESULTS AND DISCUSSIONS

A. Steady state photophysics

The AFM image of evaporated 120-nm rubrene film is displayed in [Fig. 1(a)]. The image shows that our films have a smooth surface with a root-mean-square roughness of 0.23 nm. The morphology does not exhibit either large grains or islandlike crystalline domains, which have been reported for crystalline rubrene films.^{12,13} Park *et al.*¹³ observed the growth of these domains only after annealing the films at higher-than-room temperatures, whereas our films were measured just after evaporation at room (or lower) temperatures. Furthermore, no steplike structures with step widths in the range of $1 \mu\text{m}$ or larger, characteristic of single crystal films, have been observed.^{14,15} The AFM images from our films are almost identical to the thermally evaporated amorphous rubrene film AFM image that was recorded by Seo *et al.*¹² XRD scans did not provide any peak belonging to rubrene crystal (not shown). Results from AFM and XRD measurements confirm that our rubrene films are in the amorphous phase.

The absorption spectrum of thin film [Fig. 1(b)] has three well-resolved vibronic peaks separated by 0.18 and 0.15 eV, with the highest vibronic peak at 2.33 eV. The absorption spectrum of solution is slightly blue-shifted vibronics separated by 0.17 eV, with the highest peak at 2.35 eV. The film emission spectrum peaks at 2.22 eV (559 nm), demonstrating a Stokes shift of 0.11 eV with a second vibronic ~ 2.06 eV. The emission spectrum of sublimed rubrene film is almost isoenergetic with the emission spectrum of rubrene in a dilute solution (2.23 eV).^{8,14,16,17} According to Irkhin *et al.*, who investigate absorption and photoluminescence (PL) of rubrene amorphous

and crystal films in detail,¹⁶ the highest occupied molecular orbital-to-lowest unoccupied molecular orbital transition (A_g-A_u) in rubrene occurs along the M axis [Fig. 1(b) inset], and transitions to a higher excited state (A_g-B_u) are associated with the L or N crystal direction. Their recorded PL and absorption spectra of amorphous rubrene are identical to those we recorded, both peaking at 2.22 eV with first and second vibronics in a ratio ~ 0.65 , and different from those of crystalline rubrene (cf. any crystalline rubrene spectra in Figs. 5–10 in Ref. 16). They conclude that emission in amorphous film is dominated by optical transitions along the M axis. We do not rule out the contribution of exciton states with different symmetry (N or L , transition from higher excited states) in amorphous rubrene, because the difference between the first and the second peak is 0.16 eV rather than the carbon double bond vibration of 0.18 eV. This picture is complicated by Tao *et al.*,¹⁸ who showed the existence of a self-trapped state with a depth of 35 meV in rubrene crystals arising from coupled modes of molecular deformations with phenyl side groups. It is possible that these self-trapped excitons exist in amorphous rubrene as well. We did not observe emission bands at 645 nm previously assigned to oxidation in rubrene single crystals.¹⁹ From Fig. 1(b), we assign emission recorded 2 ns after excitation to prompt fluorescence (PF), whereas emission recorded at 1600 ns is assigned to delayed fluorescence (DF) arising from triplet fusion (TF).^{6,20}

B. Femtosecond pump-probe spectroscopy

The transient absorption spectrum of rubrene is shown in Fig. 2(a) for a range of delay times. Broad, structureless photoinduced absorption (PA, $\Delta T/T < 0$) from 1.4 to 2.2 eV is identified to be induced absorption from instantaneously photoexcited hole and electron polarons. Our assignment is based on the findings by Saeki *et al.*,²¹ who recorded ground state absorption spectra of rubrene radicals (cationic and anionic), and the spectral shape of the radical absorption bands is identical to the PA between 1.4 and 2.2 eV—one broad peak between 1.6 and 2.2 eV due to the anion and

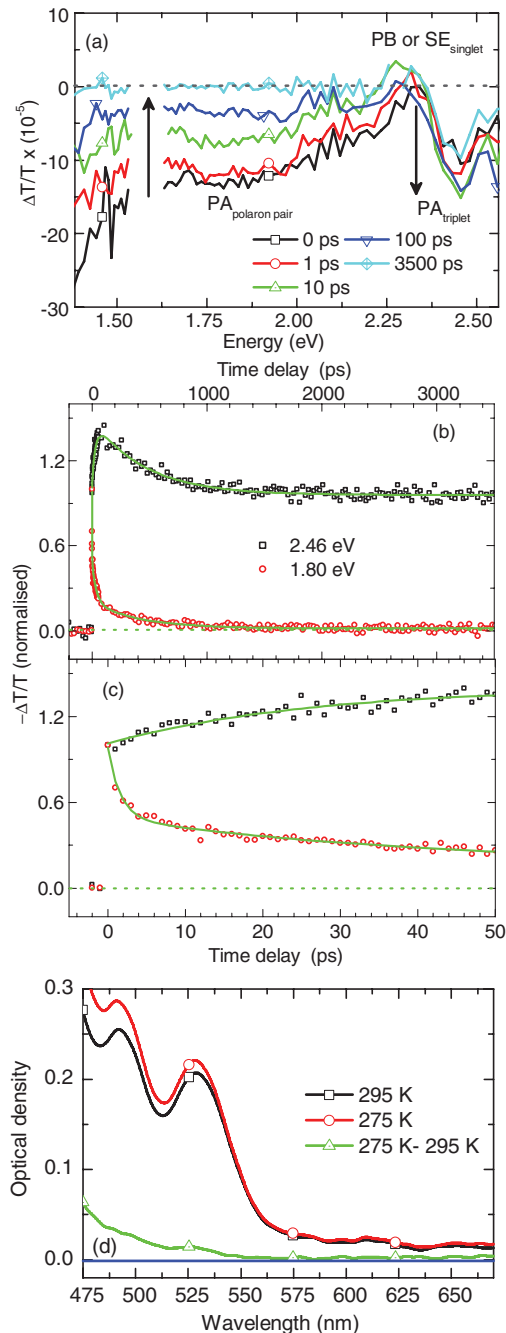


FIG. 2. (Color online) (a) Transient absorption spectra of rubrene thin film evaporated at various delay times as marked, excitation at 3.2 eV ($40 \mu\text{J cm}^{-2}$), 295 K. The band corresponding to PA ($\Delta T/T < 0$) is indicated. $\Delta T/T > 0$ was also observed and could be ascribed to either stimulated emission (SE) or photobleaching (PB). (b) Normalized transient absorption kinetics at 2.46 eV (black squares, triplet) and 1.80 eV (red circles, polaron pairs); the results of multiexponential fitting to the data are also included (green lines). Fitted triplet (2.46 eV) decay times are -30 ± 3 and 460 ± 30 ps, and fitted polaron (1.8 eV) decay times are 1.6 ± 0.1 , 36 ± 4 , and 410 ± 40 ps. (c) Close-up of the first 50 ps, highlighting the built-in component at 2.46 eV and decay at 1.80 eV. (d) Absorption spectra of rubrene film at 295 and 297 K and their subtraction. No sharp features are observed, ruling out the possibility of thermal modulation and artifacts in the transient absorption spectra. Sapphire substrates were used to help the dissipation of heat.

an onset of the narrower peak ~ 1.4 eV from the cation. Tao *et al.*,²² in rubrene single crystal, also detected a broad PA band with a shape similar to that measured here and showed excellent agreement when comparing their shape to the absorption spectra of rubrene anions and cations in solution. Tao *et al.*²² suggest that at 3.16-eV excitation energy, hot exciton dissociation in rubrene single crystals forms polaron pairs; hence, they are observed within the first few hundred femtoseconds. After excitation with 3.2 eV, we observe this band within the time resolution of our apparatus (~ 400 fs). $\Delta T/T > 0$ peaking at 2.3 eV is observed in our data, which overlaps significantly with the polaron pair PA between 2 and 2.4 eV. This could be either stimulated emission of singlet excitons or photobleaching. We suggest that polaron formation occurs from the singlet excitons within the first few hundred femtoseconds after photoexcitation. It is likely that charges are generated from higher-energy singlet excitons, as shown to happen in rubrene crystals.²² However, Tao *et al.*¹⁸ have shown that a unique path of exciton dissociation into polarons exists in rubrene crystals with the potential barrier for exciton dissociation of only 35 meV. These authors predict exciton dissociation to arise either from impurity-induced dissociation or directly from self-trapped excitons.¹⁸

A further PA band is observed between 2.3 and 2.6 eV, which is present at 0 ps and has a built-in time on the order of 10 ps. This behavior is mirrored in the properties of the polaron pair PA, which shows initial decay over the same 10-ps timescale [arrows to demonstrate this have been included in Fig. 2(a)]. This band has been identified in the literature to be the triplet PA (T_1-T_N) of rubrene and is hence assigned as thus here.^{9,23,24} We have not observed a substantial difference when subtracting the absorption spectrum recorded at 275 K from the absorption spectrum recorded at 295 K in this energy range; furthermore, the minor difference seen is positive [Fig. 2(d)]. This rules out the possibility of thermal modulation effects and artifacts in the transient absorption spectrum.²⁵ The lifetime of the triplet exciton PA is much longer than the bound polaron pair absorption; this can be readily appreciated by comparing the spectra obtained at 0 and 3500 ps, with only the triplet PA visible at 3500 ps. Multiexponential analysis of the polaron pair PA kinetics measured at 1.80 eV, presented in Fig. 2(b) and 2(c), yields decay components of 1.6 ± 0.1 , 36 ± 4 , and 410 ± 40 ps. This also confirms that the broad band between 1.4 and 2.2 eV cannot be singlet state PA, because it decays much faster than the rubrene film fluorescence with a lifetime of ~ 2 ns (see below). There is some degree of overlap between the polaron pairs and the triplet PA between 2.4 and 2.6 eV; this can be appreciated by comparing spectra in Fig. 2(a) with the spectra of rubrene anionic and cationic radicals recorded by Saeki *et al.*²¹ This matter and the effect on the transient absorption kinetics in this range are considered in more detail below.

A similar analysis of the PA kinetics at 2.46 eV [Fig. 2(b)] yields a built-in component of 30 ± 3 ps, in addition to a decay component of 460 ± 30 ps, along with the large initial PA, which arises within our time resolution. A large background offset is also recorded and is reflective of the long decay time of the triplet excitons [also discussed in context of Fig. 2(a)], which cannot be measured accurately using this apparatus. The 460-ps decay component is also identified at 1.80 eV

and ascribed to a kinetic signature of polaron pairs that arise as a consequence of the aforementioned overlap between the polaron and the triplet PA bands between 2.4 and 2.6 eV; however, from the shape of the 0-ps curve between 2.4 and 2.6 eV in Fig. 2(a), it is clear that a large triplet population is present even at these early times, meaning that triplets are created within 400 fs.

The presence of a triplet population at 0 ps indicates singlet exciton fission in these films. Intersystem crossing rates in organic molecules in the absence of metal complexes is in the range of 10^6 s^{-1} ,²⁶ whereas here the triplet formation rate is faster than $2.5 \times 10^{12} \text{ s}^{-1}$ (instrument resolution of 400 fs). Such a singlet-to-triplet conversion rate is too fast for intersystem crossing via spin-orbit coupling or through a hyperfine interaction and must arise due to singlet fission. Rates of singlet fission can range from 10^9 up to 10^{13} s^{-1} , which agrees well with our observed value.²⁷ Furthermore, given that the PL quantum yield of an isolated rubrene molecule (in dilute solution) is unity,²⁶ this implies that the molecular intersystem crossing yield (or triplet yield) must approach zero. There is no evidence to suggest a substantial intersystem crossing rate (triplet yield) increase in film, whereas the rate of singlet fission should change dramatically going from solution to solid, because at least two closely neighboring molecules are needed for two resultant triplet formation.²⁷ It is reasonable to consider that the singlet fission process arises from a higher-energy singlet state present in rubrene, as has been shown to occur in tetracene.²⁸

The matching 30-ps ($3.3 \times 10^{10} \text{ s}^{-1}$) built-in component and decay noted at 2.46 and 1.80 eV, respectively, could be interpreted in two ways. First, the 30-ps triplet built-in component, which matches the decay channel of the polaron pairs, can be ascribed to triplet formation via geminate polaron pair recombination. The data collectively presented in Fig. 2 therefore implies the direct conversion of polaron pairs to triplet excitons in rubrene, with the recorded conversion time of 30 ps characteristic of the conversion process. It is not unlikely that polaron pairs relax to triplet state; e.g., this happens in any organic light-emitting diode device when charges recombine into triplet. According to spin statistics, this could be more efficient than recombination to singlet state (3:1 triplet-singlet formation ratio). In addition, Greyson *et al.*²⁹ proposed that singlet fission into two triplets might take place via a charge transfer state, and the built-in component of the triplet band at the expense of the polaron pair band supports this view. Unfortunately, we could not record a singlet-singlet PA band in our experiments to confirm the path singlet \rightarrow polaron pair \rightarrow triplet. According to theoretical calculations by Sai *et al.*³⁰ the second rubrene singlet state is at 2.64 eV and the third is at 3.29 eV [the first is at 2.32 eV—similar to our experimental results; see Fig. 1(b)]. So S_1 - S_n transitions should be at 0.32 and 0.97 eV, and this is out of the spectral measurement window of our femtosecond system. Tao *et al.*²² observed singlet PA in their experiment—the PA bands observed at 0.37 and 1.15 eV have been assigned to singlet-singlet absorption in agreement with the calculations of Sai *et al.*³⁰

We note another possibility for the matching 30-ps built-in component and decay at 2.46 and 1.80 eV. The PA triplet band between 2.4 and 2.6 eV overlaps substantially with the ground state photobleaching of rubrene [see Fig. 1(b) for

rubrene absorption]. Hence, if polaron pairs recombine back to the singlet ground state, the photobleaching signal decreases, resulting in an overall effective increase of the PA triplet band.

To summarize the PA data, triplet excitons in rubrene are formed via a very fast (<400 fs) singlet fission process and could be formed via slower (30 ps) geminate polaron pairs recombining into triplet states (given the 30-ps rise time of the triplet band and the decay time of the polaron pair band). The presence of polaron pair bands and a triplet band at very early times (<400 fs) indicates an important role played by polaron pairs in the singlet fission process in a rubrene. But we see $\sim 75\%$ of the triplet signal within first 400 ps. Only another 25% grow in at 10 ps. It seems highly unlikely that the initial 75% is generated through the slow polaron route, so S_0 favors direct $S_1^n \rightarrow 2T_1$.

C. Nanosecond luminescence spectroscopy

To further establish the nature of the conversion process, nanosecond gated spectroscopy was employed to investigate the properties of DF (Fig. 3). Decay of rubrene film luminescence after excitation at 3.49 eV at various temperatures is depicted in Fig. 3(a) and 3(b). The exponential cascadelike feature at early times is ascribed to PF, which can be fitted with a single temperature-dependent exponent [Fig. 3(b)]. DF is a second longer-lived feature in the luminescence decay curve at all temperatures. It has been reported that DF in rubrene films arises from triplet-triplet annihilation, i.e., TF.⁶ In Fig. 3(b), the DF and PF dependence on excitation laser pulse energy is depicted. Both signals scale linearly with laser fluence. DF arising from TF normally scales quadratically with laser pulse intensity (or more correctly, with PF intensity)^{11,31} if the triplet origin is intersystem crossing from the singlet state; i.e., one singlet gives one triplet, and two triplets give back one singlet. However, if triplets are created by singlet fission and then they fuse to give back a singlet, clearly, DF arising from TF should scale linearly with initial laser energy or PF (i.e., one singlet gives two triplets and two triplets give back one singlet). This latter type of behavior is observed in our experiment in Fig. 3(b). This is a strong evidence of $S_1^n \rightarrow 2T_1$.

We do not discount that part of the DF signal in Fig. 3(a) may be due to DF arising from polaron pair recombination to yield a singlet state, since polaron pairs have been observed to be formed in Fig. 2(a). In this case, a linear DF signal dependence on pulse fluence should be expected. However, we argue that DF arises mainly from TF. First, the decay lifetime of polaron pairs is 460 ps, and it can be concluded from Fig. 2(a) that polaron pairs have already decayed long before 1 ns, whereas DF is observed up to several microseconds at room temperature. Second, there is no substantial difference between the decay recorded exciting with 3.49 and 2.33 eV [at 30 K; see Fig. 3(d)], which supports the DF origin as mainly TF. If DF arose from delayed polaron pair recombination, a lower PF/DF ratio would be expected when exciting at 2.33 eV, because less polaron pairs or charges would be created, as suggested by Tao *et al.*²² But this should not affect singlet fission as long as the excitation energy is twice of that of the triplet (1.14–1.15 eV).

It has been proposed by Zimmerman *et al.*³² that in acenes, singlet states relax to an excited dimer, which can

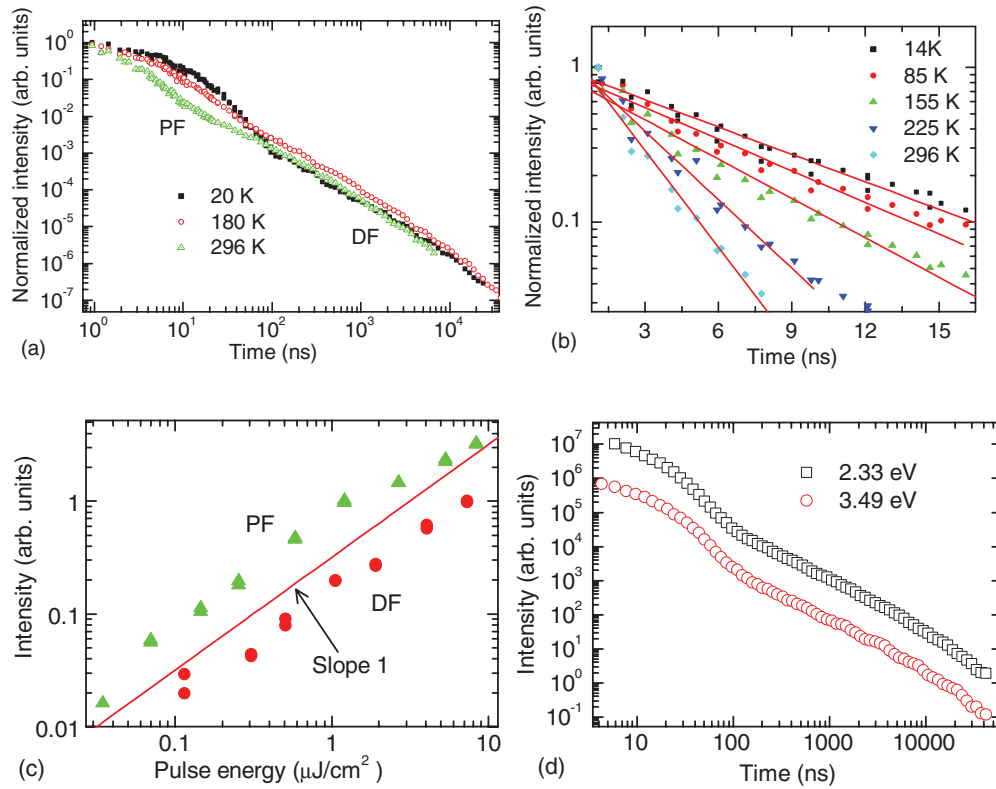


FIG. 3. (Color online) (a) Luminescence decay (normalized) of rubrene thin film at various temperatures in a log-log scale. The first cascadelike feature can be assigned to PF (exponential decay), while the second power law-like feature can be assigned to DF. (b) Log-lin scale of PF with monoexponential fittings. At later times, there is a deviation from monoexponential decay, which we ascribe to the increase of DF. (c) DF (circles) and PF (triangles) intensity dependence on laser pulse energy is linear. The straight line with the slope 1 in the log-log scale is just a visual guide. (d) Luminescence decay (corrected for optical density difference) of rubrene thin film at 30 K in a log-log scale exciting at 2.33 and 3.49 eV.

lead to a nonadiabatic transition to a multiexciton state directly connected to two localized triplets. These triplets will be close to each other, and their annihilation probability will be very high, which can lead to TF and subsequent DF. This is in line with the DF decay shape being almost independent of temperature [Fig. 3(a)]. The shape of the decay curve stays the same from 20 K to room temperature because triplets created from singlet fission are trapped on two neighboring localized sites and can undergo fusion with similar probabilities at higher or lower temperatures without any hopping through the film. This differs considerably from previous observations of triplet dynamics in polyfluorene¹¹ and *N,N'*-di(1-naphthyl)-*N,N'*-diphenylbenzidine,³¹ where triplets are generated via the intersystem crossing route. In the latter cases, the TF is hopping limited, and hence temperature dependent,^{11,31,33,34} leading to a DF decay with substantial differences at different temperatures. Normally, the change in the slope of DF decay is observed with a change of temperature due to a change from dispersive (power law with a slope of -1) to nondispersive (power law with a slope of -2) triplet exciton migration.

In Fig. 4(a), DF and PF intensity and nonradiative decay rate variations with temperature (30–300 K) are depicted. With increase of temperature, PF decreases quickly up to ~ 100 K and then stays almost constant up to 175 K. This is different behavior from that observed by Lee *et al.*³⁵

in rubrene crystal sheets with nanometer thickness. They observed slower decrease of PL with temperatures up to 100 K and faster decrease of PL from 100 to 170 K and assigned this to changes of packing in the crystal related to the motional stability of the phenyl ring torsion.³⁵ Clearly, in our amorphous film, the physics is different. To get more insight into the physics of amorphous film, we analyze DF variations with temperature [Fig. 4(a) and 4(b)]. DF changes little from 30 to 90 K, but from 100 to ~ 175 K it increases gradually, with Arrhenius activation energy of 16 meV. We ascribe this increase of DF to the increase of singlet fission efficiency subsequently giving more triplets, resulting in more DF, and assign the activation energy of singlet fission to be 16 meV. Then after a peak temperature 175 K, DF starts to decrease, with an activation energy of 36 meV. Clearly, another process becomes efficient enough to quench DF and compete with singlet fission. Tao *et al.*¹⁸ found that in crystal rubrene, the energy necessary for an exciton to escape a trapped state is 35 meV, leading to subsequent polaron creation. The agreement of activation energies is striking, especially considering the different methods used, and we conclude that at higher temperatures both DF and PF decrease for the same reason, i.e., dissociation of singlet excitons to polaron pairs. This is confirmed by PF lifetime studies.

Although from 30 to ~ 90 K PL lifetime is almost constant, it decreases with the increase of temperature above 100 K

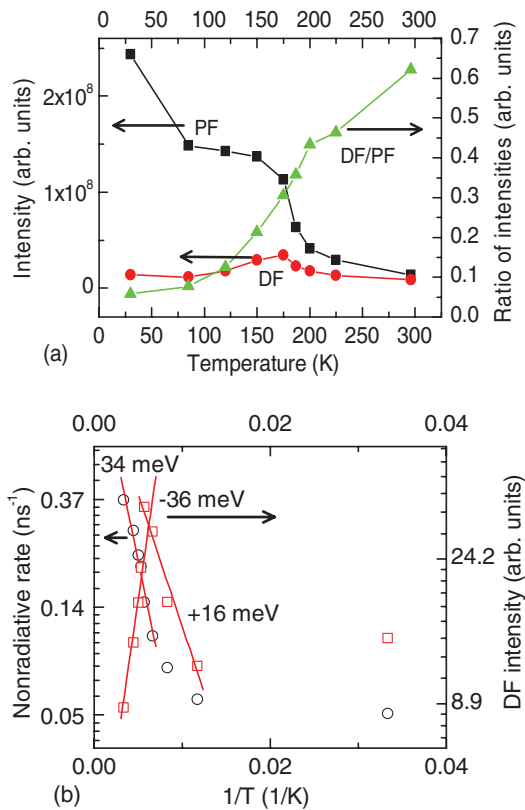


FIG. 4. (Color online) (a) Temperature dependence of DF and PF and their ratio intensity in rubrene thin film. (b) Arrhenius plots of DF intensity (squares) vs $1/T$ and nonradiative rate vs $1/T$ (circles) from rubrene thin film. The nonradiative rate in thin film was determined by subtracting the radiative rate (0.061 ns^{-1}) of rubrene (Ref. 26) from the reverse of fluorescence lifetime [Fig. 3(b)]. Numbers indicated are activation energies.

[see Fig. 3(b)]. This is characteristic of a singlet deactivation mechanism that is turned on with an increase of temperature. It is well known that the rubrene radiative rate is 16 ns^{-1} (0.061 ns^{-1}).²⁶ By knowing the PF decay lifetimes, we thus can determine the nonradiative rates at different temperatures [Fig. 4(b)]. From an Arrhenius plot fitting nonradiative PL decay vs $1/T$ from 175 to 300 K, we evaluate that the activation energy for this mechanism is 0.034 eV [Fig. 4(b)]. Again, this agrees with the energy necessary for an exciton to escape to form polarons as determined by Tao *et al.*¹⁸ DF and nonradiative decay Arrhenius analysis strongly supports femtosecond data, implying competition between singlet fission and polaron pair formation.

Here, we have to note the different physical meanings for the fission rate $>1/400 \text{ fs}^{-1}$ determined, as shown earlier, using the femtosecond pump-probe and the rate determined here using the nanosecond system; the latter is orders of magnitude smaller (e.g., $1/2.7\text{-ns}^{-1}$ fission rate at room temperature). The former is a “real” fission rate at which this process takes place, whereas the latter reflects a process during which singlet excitons can migrate to “special dimer sites” needed for singlet fission to take place, as shown by Roberts *et al.*³⁶ to take place in 5,12-diphenyltetracene. If singlet fission is $<400 \text{ fs}$, it should quench all singlet states, because the radiative rate of rubrene is 16.4 ns^{-1} .²⁶ But this does not happen,

because we observed substantial amounts of fluorescence from these films (we measured a photoluminescence quantum yield of $\sim 13\%$). Take as an example an excited state that has enough energy to achieve singlet fission but due to molecular disorder is located on a site where the rubrene dimer pair configuration is not conducive for singlet fission.^{27,29,32} Then singlet excitons have to migrate to a site where fission is more likely to take place due to a more favorable arrangement of molecules, depending on the molecular disorder; hence, a much longer lifetime for singlet fission is observed.³⁶ In this case, the limiting rate for singlet fission would be not the “real” fission rate but a rate at which the fission promoting dimer site is found via exciton migration, as observed in 5,12-diphenyltetracene previously.³⁶ This also explains why we observe different singlet fission yields at different evaporation rates when depositing films (these results will be published later).

More information can be extracted from the DF/PF ratio, which increases significantly with temperature—about tenfold from 0.05 at 30 K to almost 0.6 at room temperature [Fig. 4(a)]. DF/PF can increase only if triplet yield increases or DF yield increases. The latter does not change or decreases with temperature, because with an increase of temperature, other deactivation pathways are turned on, such as internal triplet exciton conversion or triplet quenching in nonradiative sites.^{11,31} Hence, the DF/PF ratio can increase only if triplet yield (or singlet fission) increases with temperature, again indicating the increase of singlet fission with temperature and confirming singlet hopping to the special dimer sites or the endothermic nature of this mechanism.³⁶

IV. CONCLUSIONS

We report direct evidence of singlet fission in sublimed amorphous rubrene films and measure the rubrene singlet fission rate to be $>2.5 \times 10^{12} \text{ s}^{-1}$. We also observe that triplets created by singlet fission fuse to give back a singlet, with DF scaling linearly with initial laser energy or PF (i.e., one singlet gives two triplets and two triplets give back one singlet). This is strong evidence of $S_1^0 \rightarrow 2T_1$. We evaluated that the activation energy needed for the singlet fission is 0.016 eV . We clearly show that polaron pairs are important in the singlet fission process. We found that a quenching mechanism with an activation energy of 36 meV is turned on with an increase of temperature, which we assign to proposed¹⁸ self-trapped exciton escape and dissociation into polaron pairs. The singlet state just after excitation can either relax to polaron pairs or produce two triplets; those two paths must compete with each other. It is possible that singlet fission in amorphous rubrene film takes place via a polaron pair state. It can also be inferred that some singlet excitons have to migrate to a site where fission is more likely to take place due to a more favorable arrangement, and the limiting rate for singlet fission would be not the “real” fission rate but a rate at which the fission promoting dimer site is found via exciton migration, as observed in 5,12-diphenyltetracene.³⁶ Furthermore, we observe DF in rubrene and conclude it arises from TF. We do not observe temperature dependence of DF curve shape, leading us to conclude that triplet dynamics in rubrene vacuum sublimed amorphous films is not controlled

by triplet exciton hopping. Triplets are created nearby; hence, it is easy to undergo annihilation, because there is no need to hop in films for the triplets to find each other.

ACKNOWLEDGMENT

This paper is supported by the Engineering and Physical Sciences Research Council (Grant No. EP/H051902/1).

*vygintas.jankus@durham.ac.uk

- ¹C. Silva, *Nat. Mater.* **9**, 884 (2010).
- ²H. Najafov, B. Lee, Q. Zhou, L. C. Feldman, and V. Podzorov, *Nat. Mater.* **9**, 938 (2010).
- ³J. Irkhin and I. Biaggio, *Phys. Rev. Lett.* **107**, 017402 (2011).
- ⁴J. J. Burdett, A. M. Mueller, D. Gosztola, and C. J. Bardeen, *J. Chem. Phys.* **133**, 144506 (2010).
- ⁵J. J. Burdett, D. Gosztola, and C. J. Bardeen, *J. Chem. Phys.* **135**, 214508 (2011).
- ⁶A. Ryznyanskiy and I. Biaggio, *Phys. Rev. B* **84**, 193203 (2011).
- ⁷L. Ma, K. K. Zhang, C. Kloc, H. D. Sun, M. E. Michel-Beyerle, and G. G. Gurzadyan, *Phys. Chem. Chem. Phys.* **14**, 8307 (2012).
- ⁸T. Petrenko, O. Krylova, F. Neese, and M. Sokolowski, *New J. Phys.* **11**, 015001 (2009).
- ⁹F. Lewitzka and H. G. Löhmannsröben, *Z. Phys. Chem.* **150**, 69 (1986).
- ¹⁰W. G. Herkstroeter and P. B. Merkel, *J. Photochem.* **16**, 331 (1981).
- ¹¹C. Rothe and A. P. Monkman, *Phys. Rev. B* **68**, 075208 (2003).
- ¹²J. H. Seo, D. S. Park, S. W. Cho, C. Y. Kim, W. C. Jang, C. N. Whang, K.-H. Yoo, G. S. Chang, T. Pedersen, A. Moewes, K. H. Chae, and S. J. Cho, *Appl. Phys. Lett.* **89**, 163505 (2006).
- ¹³S.-W. Park, J.-M. Choi, K. H. Lee, H. W. Yeom, S. Im, and Y. K. Lee, *J. Phys. Chem. B* **114**, 5661 (2010).
- ¹⁴X. Zeng, D. Zhang, L. Duan, L. Wang, G. Dong, and Y. Qiu, *Appl. Surf. Sci.* **253**, 6047 (2007).
- ¹⁵P. Zhang, X. Zeng, J. Deng, K. Huang, F. Bao, Y. Qiu, K. Xu, and J. Zhang, *Jpn. J. Appl. Phys.* **49**, 095501 (2010).
- ¹⁶P. Irkhin, A. Ryznyanskiy, M. Koehler, and I. Biaggio, *Phys. Rev. B* **86**, 085143 (2012).
- ¹⁷L. Huang, Q. Liao, Q. Shi, H. Fu, J. Ma, and J. Yao, *J. Mater. Chem.* **20**, 159 (2010).
- ¹⁸S. Tao, N. Ohtani, R. Uchida, T. Miyamoto, Y. Matsui, H. Yada, H. Uemura, H. Matsuzaki, T. Uemura, J. Takeya, and H. Okamoto, *Phys. Rev. Lett.* **109**, 097403 (2012).
- ¹⁹O. Mitrofanov, C. Kloc, T. Siegrist, D. V. Lang, W.-Y. So, and A. P. Ramirez, *Appl. Phys. Lett.* **91**, 212106 (2007).
- ²⁰C. Rothe, R. Guentner, U. Scherf, and A. P. Monkman, *J. Chem. Phys.* **115**, 9557 (2001).
- ²¹A. Saeki, S. Seki, T. Takenobu, Y. Iwasa, and S. Tagawa, *Adv. Mater.* **20**, 920 (2008).
- ²²S. Tao, H. Matsuzaki, H. Uemura, H. Yada, T. Uemura, J. Takeya, T. Hasegawa, and H. Okamoto, *Phys. Rev. B* **83**, 075204 (2011).
- ²³A. Yildiz, P. T. Kissinger, and C. N. Reilly, *J. Chem. Phys.* **49**, 1403 (1968).
- ²⁴D. K. K. Liu and L. R. Faulkner, *J. Am. Chem. Soc.* **99**, 4594 (1977).
- ²⁵A. Rao, M. W. B. Wilson, S. Albert-Seifried, R. Di Pietro, and R. H. Friend, *Phys. Rev. B* **84**, 195411 (2011).
- ²⁶J. B. Birks, *The Photophysics of Aromatic Molecules* (John Wiley & Sons, London, 1970).
- ²⁷M. B. Smith and J. Michl, *Chem. Rev.* **110**, 6891 (2010).
- ²⁸V. K. Thorsmølle, R. D. Averitt, J. Demsar, D. L. Smith, S. Tretiak, R. L. Martin, X. Chi, B. K. Crone, A. P. Ramirez, and A. J. Taylor, *Phys. Rev. Lett.* **102**, 017401 (2009).
- ²⁹E. C. Greyson, J. Vura-Weis, J. Michl, and M. A. Ratner, *J. Phys. Chem. B* **114**, 14168 (2010).
- ³⁰N. Sai, M. L. Tiago, J. R. Chelikowsky, and F. A. Reboredo, *Phys. Rev. B* **77**, 161306 (2008).
- ³¹V. Jankus, C. Winscom, and A. P. Monkman, *J. Phys. Condens. Matter* **22**, 185802 (2010).
- ³²P. M. Zimmerman, F. Bell, D. Casanova, and M. Head-Gordon, *J. Am. Chem. Soc.* **133**, 19944 (2011).
- ³³M. Scheidler, B. Cleve, H. Bassler, and P. Thomas, *Chem. Phys. Lett.* **225**, 431 (1994).
- ³⁴A. Kohler and H. Bassler, *Mater. Sci. Eng. R* **66**, 71 (2009).
- ³⁵J. W. Lee, S. G. Jo, J. Joo, J. H. Kim, and H. Rho, *Phys. Rev. B* **86**, 075416 (2012).
- ³⁶S. T. Roberts, R. E. McAnally, J. N. Mastron, D. H. Webber, M. T. Whited, R. L. Brutchey, M. E. Thompson, and S. E. Bradforth, *J. Am. Chem. Soc.* **134**, 6388 (2012).